

Diffuse X-ray streaks from stacking faults in Si analyzed by atomistic simulations

K. Nordlund

Accelerator Laboratory, P.O. Box 43, FIN-00014 University of Helsinki, Finland

U. Beck and T. H. Metzger

Sektion Physik and Center for NanoScience (CeNS), LMU München, Geschwister-Scholl-Platz 1, D-80539 München, Germany

J. R. Patel

SSRL/SLAC, Stanford University, Stanford, CA 94309, USA

ALS/LBL, 1 Cyclotron Road, Berkeley, CA 94720, USA

(December 20, 1999)

Since extrinsic stacking faults can form during post-implantation annealing of Si, understanding their properties is important for reliable control of semiconductor manufacturing processes. We demonstrate how grazing incidence X-ray scattering methods can be used as a nondestructive means for detecting extrinsic stacking faults in Si. Atomistic analysis of diffuse intensity streaks is used to determine the size of the faults, the minimum size at which the streak pattern in the scattering will be visible, and the magnitude of atomic displacements in the center of the stacking fault.

Ion implantation of silicon and subsequent high-temperature annealing plays a central role in present-day semiconductor manufacturing. Although the overall development of the implantation damage production and annealing is relatively well understood^{1,2}, many details remain unclear. The analysis of defect states during annealing is usually done using transmission electron microscopy. Although the method has many advantages, it works only for very thin samples, and it is possible that the sample thinning process affects the nature of the defects in the sample. Hence it could be very useful to have complementary methods for analyzing the nature of defects in Si.

The “diffuse” X-ray scattering distribution from a defective crystal is the weak part of the scattering between Bragg peaks which arises from the strain field in the lattice surrounding the defects. The diffuse X-ray scattering (DXS) method is a fast and nondestructive means to analyze damage in lattices, such as point and extended defects^{3,4}. Although the method has been much used for metals^{5,6}, its application to semiconductors has been hampered by the difficulty of analyzing the results. Nordlund *et al.* have recently developed a method enabling atomistic simulations of DXS measurements even for very complex defect configurations. We have found that the using the method it is, at least in principle, possible to distinguish different interstitial and vacancy configurations⁷, determine the size of vacancy and interstitial clusters in semiconductors, and the average separation between interstitial- and vacancy-like defects⁸.

Here we will describe how the atomistic analysis method can be used for detection of stacking faults in Si, and use the method to determine the average size and the magnitude of atomic displacements of stacking faults formed in boron implanted Si after thermal processing.

For the measurements of the diffuse x-ray scattering we have applied the geometry of grazing incidence and exit⁹, which allows accurate control of the scattering depth

by choosing values for the incidence angle α_i and the exit angle α_f close to the critical angle of total external reflection α_c ¹⁰. Thus we could probe the near surface region affected by the implantation process. The vicinity of surface reflections with scattering planes perpendicular to the sample surface were investigated.

For data collection a one-dimensional position sensitive detector (PSD) was used, which could be operated in two different modes. The PSD is placed parallel to the sample surface at a fixed exit angle. Thus the vicinity of the surface peak could be mapped in terms of a Q_x - Q_y -plane of reciprocal space at constant Q_z . In the perpendicular mode the PSD is normal to the sample surface, so that $Q_{||}$ - Q_z mappings could be efficiently recorded. The details of the measurement procedure are described elsewhere¹¹.

Dislocation free, floating-zone Si (001) single crystals were implanted with 32 keV boron to a boron dose of 6×10^{15} ions/cm². The implanted samples were rapid thermal annealed at 1070 °C for 10 seconds.

The resulting scattering pattern is illustrated in Fig. 1. The streaks observed along $\langle 111 \rangle$ directions in the experiments are quite similar to the streaks predicted to arise from bound stacking faults (Frank loops) in face-centered cubic metals⁴. Also, previous transmission electron microscopy studies of boron implanted and annealed Si as well as annealed silicon with high oxygen content show extrinsic Frank type stacking faults¹². This strongly suggests that the streaks now seen in Si arise from extrinsic stacking faults produced by interstitials precipitating on $\{111\}$ planes. To gain certainty of this, and enable a more detailed analysis than that provided by the traditional analytical and numerical methods, we used the new atomistic method^{8,7} to simulate DXS from stacking faults in Si.

In the atomistic analysis method of Nordlund, Partyka and Averbach^{8,7}, the DXS from a defect is calculated by forming the atom coordinates of a defect, and surrounding it by a large sphere (usually having of the

order of 1 - 100 million atoms) of undisturbed lattice atoms. All the atoms in this sphere are relaxed to the closest potential energy minimum by an efficient adaptive-step conjugate gradient method, which gives the strain field surrounding the defect⁸. The potential energy of the system is calculated from a classical interatomic potential known to describe the elastic properties of the material well. The X-ray scattering intensity $S(\mathbf{K})$ can then be calculated from the relaxed atom cell by straightforward summation over atom coordinates \mathbf{R}_i ,

$$S(\mathbf{K}) = \left| f_{\mathbf{K}} \sum_i e^{-\sigma^2 \mathbf{R}_i^2 / 2a^2} e^{i\mathbf{K} \cdot \mathbf{R}_i} \right|^2, \quad (1)$$

where σ is a convolution factor speeding up convergence of the sum, a the lattice constant and $f_{\mathbf{K}}$ is the atomic form factor^{3,13,14}. Although the atomistic analysis scheme requires large computer capacity, it has the advantage that once it is implemented, the same method can be used to deal with any kind of defect, including very complex ones. Additional details of the method are given elsewhere^{8,7}.

We created interstitial loop (extrinsic stacking fault) configurations of different sizes by adding an extra double (111) atom plane¹⁵ in the center of a large atomistic simulation cell. The extra plane had the shape of either a regular triangle or a regular hexagon bound by dislocation line segments along (110) crystal directions. To study size effects, we used lengths between 8 and $20 \frac{1}{2}(110)a$ (a is the lattice constant) for one side of the triangle or hexagon, corresponding to between 72 (for the 8-sided triangle), and 2282 (for the 20-sided hexagon) extra atoms in the stacking fault. The X-ray scattering was then calculated using the method outlined above, using spheres with radii of at least 200 Å. The well-tested Stillinger-Weber¹⁶ and Tersoff III¹⁷ force models were used to describe the potential energy of the atoms.

Figure 2 illustrates the simulated streaks produced by a hexagonal stacking fault with a side length of $14 \frac{1}{2}(110)a$, averaged over all four possible stacking fault orientations. The reason that the simulated $\langle \bar{1}\bar{1}1 \rangle$ streak appears to have a peak is the presence of zero-intensity nodal points similar to those reported in metals⁴. The strong streak in the $\langle 111 \rangle$ direction (upper right) and the somewhat weaker streak seen in the $\langle \bar{1}\bar{1}1 \rangle$ direction are very similar to those seen in the experiments. The iso-intensity contours are not quite equal in shape because we were not able to simulate as large loops as those present in the experiment, or the scattering quite as close to the Bragg peak. But as we shall see below, we were still able to give a size estimate for the defects.

Although the basic features of the scattering are thus the same as those predicted by numerical methods⁴, the atomistic analysis method allowed us to quantitatively examine atomistic effects in the scattering. The inset in Fig. 2 shows iso-intensity contours for the scattering from stacking fault triangles of varying sizes. The results show that the characteristic streak pattern becomes visible between side lengths of 8 and $16 \frac{1}{2}(110)a$, i.e. when the number of interstitial atoms in the fault is in the range

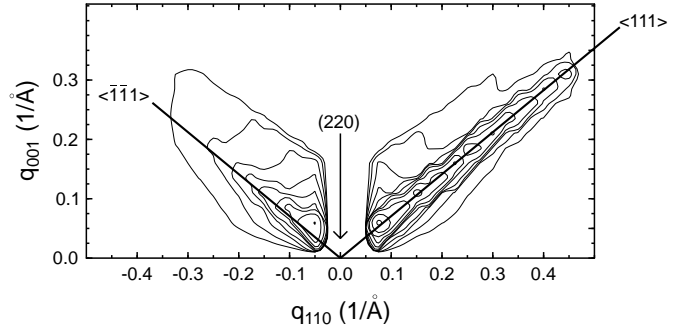


FIG. 1. Streaked X-ray scattering pattern along $\langle 111 \rangle$ from B implanted Si after a 10 s anneal at 1070 °C. q_{110} indicates the distance from the (220) Bragg peak in reciprocal space along the 110 direction and q_{001} in the vertical 001 direction. Because of experimental limitations the $|q_{110}| \lesssim 0.03$ 1/Å region in reciprocal space was not measured.

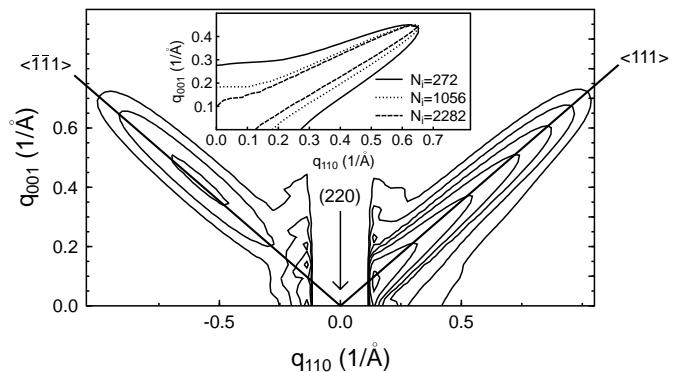


FIG. 2. As Figure 1, but with a simulated DXS pattern from a stacking fault formed by about 1000 interstitial atoms. Because we were not able to simulate as large faults as the experimental ones, the plotting range is different from that in the experimental figure. The pattern is averaged over the four equivalent orientations of a $\{111\}$ stacking fault. The inset shows one iso-intensity curve on the positive side of the (220) peak for three stacking faults with different numbers of interstitial atoms N_i . The scattering pattern is qualitatively very similar to the experimental pattern, with a strong scattering streak extending along the $\langle 111 \rangle$ direction and a somewhat weaker streak in the $\langle \bar{1}\bar{1}1 \rangle$ direction. The inset shows that as the stacking fault size grows the streak will become narrower.

100 – 200. Comparison of the streak shapes and widths for triangular and hexagonal faults further showed that the scattering pattern is very similar when the number of atoms in the fault is the same, i.e. that the streak shape is not sensitive to the exact shape of the loop.

We further used the atomistic simulations to test Vaclav Holý's analytical model for the width of the $\langle 111 \rangle$ streaks¹¹. The model predicts the shape of the scattering for a circular Frank loop of diameter d . When we defined the effective diameter d^* of a hexagonal stacking fault to be the average of the major and minor axes (i.e. $d^* = 1 + \sqrt{3}/2)l$, where l is the length of one side), we obtained excellent agreement between Holý's model and the simulations. This shows that Holý's model can be used to give a reliable size estimate even for non-circular loops. Using Holý's model to analyze the experimental data showed that the average effective diameter d^* of the

stacking faults in Fig. 1 is 710 Å.

Analysis of the experimental intensity profile along the $\langle 111 \rangle$ direction along the streak shows a characteristic crossover between $1/q^2$ and $1/q^4$ -dependence of the intensity (q is the distance to the Bragg peak in reciprocal space), similar to that occurring for large defect clusters⁶. The experimental value for the crossover point is 0.34 1/Å (Fig. 3). The simulations showed that the location of this crossover is independent of the diameter of the loop over the entire size range examined. This indicates that the crossover must be related to the “strength” of the stacking fault, i.e. the thickness of the fault and the displacements of the atoms in the center of the fault.

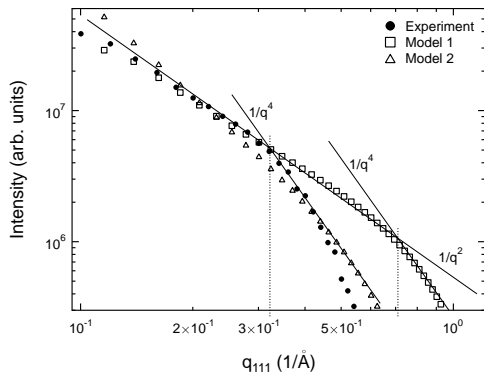


FIG. 3. Scattering intensity along the $[111]$ direction off the (220) Bragg peak. The straight solid lines indicate perfect $1/q^2$ and $1/q^4$ dependence of the scattering, and the vertical dotted lines the location of the crossover between $1/q^2$ and $1/q^4$ behaviour. The two different simulation models are calculated for stacking faults which have exactly the same shape and numbers of interstitial atoms, but different displacements in the stacking fault plane.

To further examine this, we simulated DXS from the same stacking fault with different displacements in the center of the fault. Since most Si interatomic potentials only have nearest-neighbour interactions, and all atoms in the center of a perfect stacking fault in Si have the ideal nearest-neighbour environment, the potentials give a stacking fault energy of zero, and thus no atomic displacements due to the incorrect stacking sequence of the diamond lattice¹⁸. Therefore we modified the length scale of the Stillinger-Weber (SW) interatomic potential for the atoms in the stacking fault center to be able to examine the effect of the atomic displacements on the $1/q^2 - 1/q^4$ - crossover. The tested modifications ranged from a 2 – 8 % increase in the nearest-neighbour separation and cutoff distance. The atoms outside the stacking fault center were still described by the ordinary SW potential, ensuring that the long-range strain field is realistic. The results are shown in Fig. 3. “Model 1” is the plain SW potential scattering. The location of the crossover was found to be reproduced well by models for which the average separation between double (111) atom layers (counted along the nearest-neighbour atom bond separating the layers) at and next to the stacking fault center plane was $2.42 \pm 0.02 \text{ Å}$. One of these models is shown as “Model 2” in Fig. 3. In the present case

a more accurate determination of the displacements was not possible due to the artificial nature of the potential modification, but we note that with the method outlined here it will be possible to determine the displacements accurately when Si force models with realistic long-range interactions become available, or alternatively to test candidates for such models.

In conclusion, using diffuse X-ray scattering methods, we have detected extrinsic stacking faults in boron-implanted Si after a rapid-thermal anneal. We have further shown how atomistic analysis of X-ray scattering experiments can be used to determine the size of the fault and the magnitude of atomic displacements in the stacking fault plane.

The research was supported by the Academy of Finland under projects No. 45481 and 44215, and by the Deutsche Forschungsgemeinschaft project number PE 127/4. Grants of computer time from the Center for Scientific Computing in Espoo, Finland are gratefully acknowledged.

- ¹ D. J. Eaglesham, P. A. Stolck, H.-J. Gossmann, T. E. Haynes, and J. M. Poate, Nucl. Instr. Meth. Phys. Res. B **106**, 191 (1995).
- ² E. Chason, S. T. Picraux, M. Poate, J. O. Borland, M. I. Current, T. Diaz de la Rubia, D. J. Eaglesham, O. W. Holland, M. E. Law, C. W. Magee, J. W. Mayer, J. Melngailis, and A. F. Tasch, J. Appl. Phys **81**, 6513 (1997).
- ³ P. H. Dederichs, J. Phys. F: Metal Phys. **3**, 471 (1973).
- ⁴ P. Ehrhart, H. Trinkaus, and B. C. Larson, Phys. Rev. B **25**, 834 (1982).
- ⁵ H. Dosch, U. Schubert, H. Metzger, and J. Peisl, J. Phys. F: Met. Phys. **14**, 2467 (1984).
- ⁶ P. Ehrhart and R. S. Averback, Phil. Mag. A **60**, 283 (1989).
- ⁷ P. J. Partyka, K. Nordlund, I. K. Robinson, R. S. Averback, and P. Ehrhart, unpublished.
- ⁸ K. Nordlund, P. Partyka, and R. S. Averback, in *Defects and Diffusion in Silicon Processing*, Vol. 469 of *MRS Symposium Proceedings*, edited by T. Diaz de la Rubia, S. Coffa, P. A. Stolck, and C. S. Rafferty (Materials Research Society, Pittsburgh, 1997), pp. 199–204.
- ⁹ T. Salditt, T. H. Metzger, and J. Peisl, Phys. Rev. Lett. **73**, 2228 (1994).
- ¹⁰ H. Dosch, Phys. Rev. B **35**, 2137 (1987).
- ¹¹ U. Beck, T. H. Metzger, K. Nordlund, V. Holý, and J. Peisl, unpublished.
- ¹² D. M. Maher, A. Staudinger, and J. R. Patel, J. Appl. Phys. **47**, 3813 (1976), K. S. Jones, K. Liu, L. Zhang, V. Krishnamoorthy, R.T DeHoff, Nucl. Instr. Meth. Phys. Res. B **106**, 227 (1995).
- ¹³ D. T. Keating and A. N. Goland, Acta Cryst. A **27**, 134 (1971).
- ¹⁴ In the present analysis we neglect the atomic form factor for simplicity. Its inclusion would not affect the conclusions significantly.
- ¹⁵ J. P. Hirth and J. Lothe, *Theory of dislocations*, 2nd ed. (Krieger, Malabar, Florida, 1992).
- ¹⁶ F. H. Stillinger and T. A. Weber, Phys. Rev. B **31**, 5262 (1985).
- ¹⁷ J. Tersoff, Phys. Rev. B **38**, 9902 (1988).
- ¹⁸ J. F. Justo, M. Z. Bazant, E. Kaxiras, V. V. Bulatov, and S. Yip, Phys. Rev. B **58**, 2539 (1998).